

Article

## An Improved CO<sub>2</sub> Separation and Purification System Based on Cryogenic Separation and Distillation Theory

Gang Xu, Feifei Liang, Yongping Yang \*, Yue Hu, Kai Zhang and Wenyi Liu

Beijing Key Laboratory of Emission Surveillance and Control for Thermal Power Generation, School of Energy Power & Mechanical Engineering, North China Electric Power University, Beijing 102206, China; E-Mails: xgncepu@163.com (G.X.); liangffncepu@126.com (F.L.); hy8626566@163.com (Y.H.); kzhang@ncepu.edu.cn (K.Z.); lwy@ncepu.edu.cn (W.L.)

\* Author to whom correspondence should be addressed; E-Mail: yypncepu@163.com; Tel.: +86-10-61772011.

Received: 4 March 2014; in revised form: 29 April 2014 / Accepted: 14 May 2014 /

Published: 23 May 2014

---

**Abstract:** In this study, an improved CO<sub>2</sub> separation and purification system is proposed based on in-depth analyses of cryogenic separation and distillation theory as well as the phase transition characteristics of gas mixtures containing CO<sub>2</sub>. Multi-stage compression, refrigeration, and separation are adopted to separate the majority of the CO<sub>2</sub> from the gas mixture with relatively low energy penalty and high purity. Subsequently, the separated crude liquid CO<sub>2</sub> is distilled under high pressure and near ambient temperature conditions so that low energy penalty purification is achieved. Simulation results indicate that the specific energy consumption for CO<sub>2</sub> capture is only 0.425 MJ/kgCO<sub>2</sub> with 99.9% CO<sub>2</sub> purity for the product. Techno-economic analysis shows that the total plant investment is relatively low. Given its technical maturity and great potential in large-scale production, compared to conventional MEA and Selexol™ absorption methods, the cost of CO<sub>2</sub> capture of the proposed system is reduced by 57.2% and 45.9%, respectively. The result of this study can serve as a novel approach to recovering CO<sub>2</sub> from high CO<sub>2</sub> concentration gas mixtures.

**Keywords:** CO<sub>2</sub> recovery; cryogenic separation; conventional distillation; techno-economic analysis; oxy-fuel combustion

---

## 1. Introduction

One of the most sophisticated challenges in environmental protection in the 21st century is global warming, which is caused by large amounts of greenhouse gas emissions, especially CO<sub>2</sub>. Measures must be taken to reduce CO<sub>2</sub> emissions and consequently restrain global warming. From the perspective of energy utilization, carbon capture and storage (CCS) is considered to be one of the most significant methods in CO<sub>2</sub> reduction [1], since it is reported that 90% of CO<sub>2</sub> emissions are generated by the combustion of fossil fuels, which will be extensively used in the foreseeable future [2].

Currently, several primary CO<sub>2</sub> capture and recovery methods are available: absorption (including chemical absorption and physical absorption), adsorption, membrane separation, and cryogenic separation [3–5]. Among these methods, chemical absorption can separate large amounts of high purity CO<sub>2</sub> from low concentration flue gas, but high energy penalty and huge investments are expected [5–7]. Physical absorption is an effective approach to recovering low purity CO<sub>2</sub> with low energy penalty, but additional energy is needed for sequent compression because the separated CO<sub>2</sub> is in the gas state [7–9]. Both absorption methods draw extensive attention because of their high technical maturity [5–9]. Adsorption and membrane separation are recognized as promising CO<sub>2</sub> capture methods despite inevitable problems such as low processing ability and high investment because of their operational feasibility and low separation energy penalty [10–16].

Cryogenic separation is a physical process that separates CO<sub>2</sub> under extremely low temperature. It enables direct production of liquid CO<sub>2</sub> at a low pressure, so that the liquid CO<sub>2</sub> can be stored or sequestered via liquid pumping instead of compression of gaseous CO<sub>2</sub> to a very high pressure, thereby saving on compression energy [17–20]. During the cryogenic separation process, the components of gas mixtures are separated by a series of compression, refrigeration, and separation steps. Since all these steps are highly mature technologies in the chemical industry, their operation and design feasibility can be guaranteed [20–22]. The cryogenic separation process requires no chemical agent, hence avoiding secondary pollution [17–22]. As far as industrial application is concerned, gas mixtures are usually composed of CO<sub>2</sub> and other gases, the boiling points of which are relatively low. These gases include H<sub>2</sub>, N<sub>2</sub>, O<sub>2</sub>, Ar, and CH<sub>4</sub>. These impurities lower the phase transition temperature of CO<sub>2</sub>, which can even drop to under –80 °C. In this case, the refrigeration energy penalty increases substantially, and CO<sub>2</sub> frost formation becomes highly possible, thereby threatening equipment safety [23]. Attention should thus be paid to raising the phase transition temperature of CO<sub>2</sub> to improve the cryogenic separation method and consequently avoid facility freezing problems and high energy penalty [24–27].

Recently, many studies concerning cryogenic CO<sub>2</sub> separation methods have been conducted. For instance, Besong *et al.* [28] proposed a cryogenic liquefaction system whose mainstay is formed by compressor and flash unit, so the energy penalty decreases due to sufficient recovery of cold energy. Song *et al.* [29] developed a novel CO<sub>2</sub> capture process based on a Stirling cooler, whereby CO<sub>2</sub> is separated in liquid state after continuous cooling down by three Stirling coolers. Jana [30] researched the integration and optimization of a CO<sub>2</sub> capture system, and discussed the influences of several parameters on system performance. Based on the phase transition mechanism and the principle of energy cascade utilization, in a previous work we presented a novel system that simultaneously fulfills CO<sub>2</sub> separation and compression by adopting multi-stage compression and separation. Compared with conventional CO<sub>2</sub>

capture methods, this novel system shows superior performance with CO<sub>2</sub>-H<sub>2</sub> mixture and reduces the CO<sub>2</sub> recovery energy penalty by 65% and 15%, respectively [31].

Interestingly, the studies mentioned above mainly focus on achieving high CO<sub>2</sub> capture rates and low recovery energy penalties, whereas little attention is paid to the purity of the captured CO<sub>2</sub>. In fact, CO<sub>2</sub> purity in the product separated by the cryogenic separation method might be relatively low. For example, when applying the cryogenic separation method to separate CO<sub>2</sub> from CO<sub>2</sub>-N<sub>2</sub>-O<sub>2</sub>-Ar mixtures, the impurity content in the separated liquid can be as high as 2% to 5%; at this level, the CO<sub>2</sub> purity cannot satisfy the requirements of most industrial applications, as well as transport and storage [1,32,33].

In the present work, we propose an improved CO<sub>2</sub> separation and purification system that can separate the majority of the CO<sub>2</sub> in liquid state from the mixed gases with relatively low energy penalty via multi-stage compression, refrigeration, and separation. Furthermore, by introducing high pressure and near ambient temperature distillation into the improved system, CO<sub>2</sub> purity in the final product reaches 99.9%.

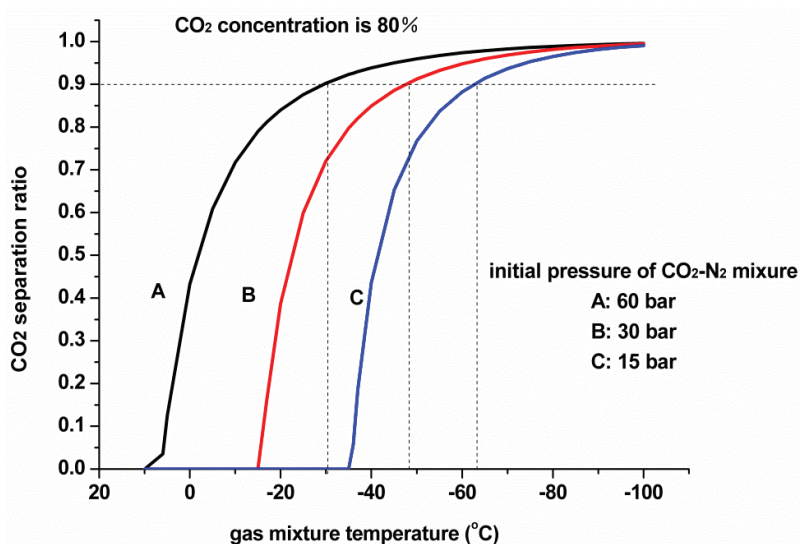
## 2. Proposal of the Cryogenic Separation Method

### 2.1. Phase Transition Characteristics of Mixed Gases Containing CO<sub>2</sub>

In our previous works, the phase transition characteristics of CO<sub>2</sub>-H<sub>2</sub> mixture (common in the syngas generated by shift reaction) were analyzed. Results indicate that CO<sub>2</sub> separation ratio is determined by two critical factors: the initial CO<sub>2</sub> concentration and the initial pressure of the gas mixture [31]. In the present study, we analyze the CO<sub>2</sub>-N<sub>2</sub>-O<sub>2</sub>-Ar mixture, which is common in oxy-fuel combustion.

Figure 1 presents the relationship between the CO<sub>2</sub> separation ratio and the temperature of CO<sub>2</sub>-N<sub>2</sub> mixtures under different initial pressures, at an initial CO<sub>2</sub> concentration of 80%.

**Figure 1.** Variation in the initial pressure and CO<sub>2</sub> separation ratio of CO<sub>2</sub>-N<sub>2</sub> with temperature.



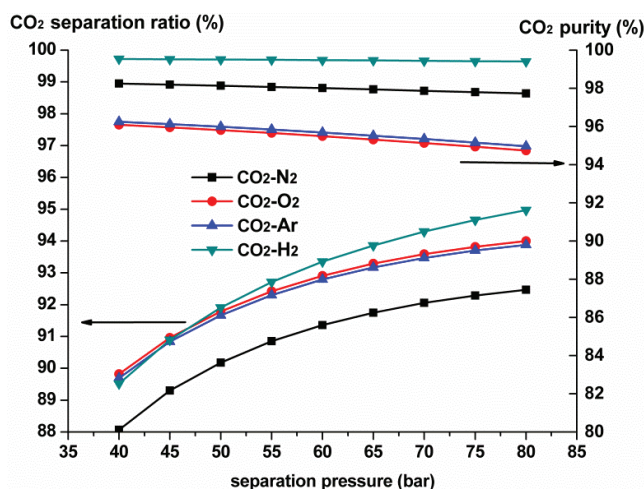
The CO<sub>2</sub> separation ratio increases as the initial pressure rises. Under the initial pressures of 15, 30, and 60 bar, to separate 90% CO<sub>2</sub> from the gas mixture, the temperature must be dropped to approximately -63 °C, -48 °C, and -30 °C, respectively, so increasing the initial pressure is an

effective approach for improving the performance of the cryogenic separation method. Especially after the gas mixture enters the cryogenic CO<sub>2</sub> separation unit, the CO<sub>2</sub> concentration in the gas mixture continuously declines with CO<sub>2</sub> condensation. If the total pressure of the gas mixture could be increased at this moment, then CO<sub>2</sub> partial pressure will also increase, which is very important in maintaining the liquefaction temperature of CO<sub>2</sub> at a high level.

## 2.2. CO<sub>2</sub> Purity Characteristics of the Cryogenic Separation Method

Generally, a small amount of impurities always dissolve in the liquid CO<sub>2</sub> separated under high pressure, and the higher separation pressure, the larger the amount of impurities [28]. Figure 2 shows the variation in CO<sub>2</sub> purity and separation ratio under different separation pressures with four kinds of typical impurity compositions, at the initial CO<sub>2</sub> concentration of 80%. The following conclusions can be drawn based on Figure 2. On the one hand, the CO<sub>2</sub> separation ratio constantly increases with the increment of separation pressure, whereas the CO<sub>2</sub> purity in the product decreases. On the other hand, different impurity compositions have different effects on the CO<sub>2</sub> purity in the product. At the same separation pressure of 60 bar and initial CO<sub>2</sub> concentration of 80%, the CO<sub>2</sub> purity in the product of the CO<sub>2</sub>-H<sub>2</sub> mixture is 99.47%, for the CO<sub>2</sub>-N<sub>2</sub> mixture it's 98.01%, whereas for CO<sub>2</sub>-O<sub>2</sub> and CO<sub>2</sub>-Ar mixtures, it sharply reduces to 95.5% and 95.69%, respectively. This is because there exist significant differences in the physical properties of the different impurity gases, which affect the thermodynamic properties such as dew and bubble points, heat capacity, enthalpy and entropy of the CO<sub>2</sub> mixture, so the operating conditions and separation performance of the purification process will thus vary accordingly, resulting in different CO<sub>2</sub> purity in the product [27]. Generally, if the physical properties of the impurity gas are distinguished from those of the CO<sub>2</sub> (H<sub>2</sub> for example), it is easier to separate them by high pressure cryogenic separation [31]. However, for gas mixtures consisting of CO<sub>2</sub>, N<sub>2</sub>, O<sub>2</sub>, and Ar, the CO<sub>2</sub> purity in the product attained by high pressure cryogenic separation is too low to satisfy the requirements of most industrial applications as well as transport and storage. Further purification measures should thus be considered.

**Figure 2.** Variation in CO<sub>2</sub> purity and separation ratio with different separation pressures and impurity compositions.

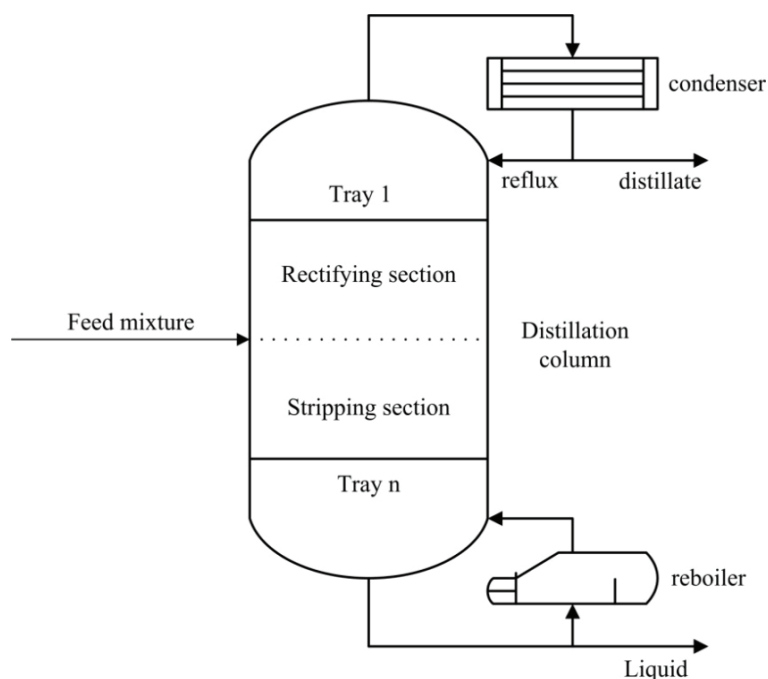


### 3. Distillation Mechanism and Feasibility Analysis

#### 3.1. Distillation Mechanism

Distillation, which is the workhorse of chemical process industries, is widely used because of its high technical maturity [34,35]. It separates gas or liquid mixtures via consecutive partial vaporization and condensation in a distillation column. Figure 3 illustrates a simplified layout of the conventional distillation process. A feed mixture enters the column from the intermediate section. After condensing by the condenser installed on top of the column, part of the condensed liquid is refluxed, while the rest is discharged as distillate. Generally, the feed entrance divides the distillation column into two sections. The upper section is called the rectifying section, where the rising steam passes through the trays and comes in contact with the refluxed liquid to realize the material transfer and densification of volatile components [36]. Underneath the entrance is the stripping section, where the steam is heated by the reboiler located at the bottom of the column. Energy and material transfer proceeds as long as the heated steam is in countercurrent contact with the descending liquid, thus resulting in the accumulation of involatile components at the bottom.

**Figure 3.** Typical layout of the conventional distillation process.



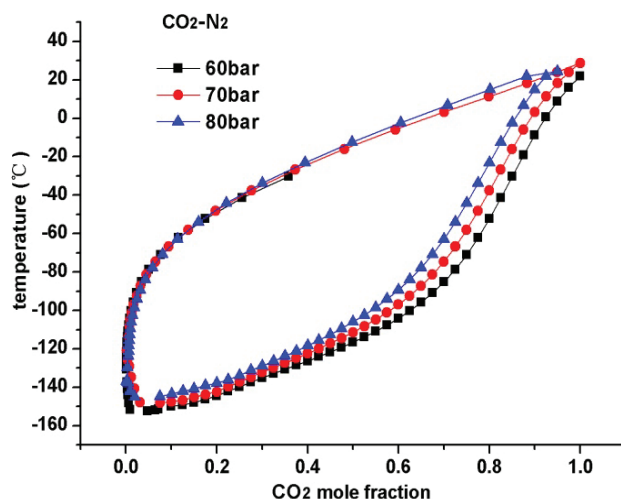
#### 3.2. Feasibility Analysis of Purifying CO<sub>2</sub> Mixture by Conventional Distillation

Certain conditions must be met when using conventional distillation to purify a mixture. In general, the basic condition lies in the difference in the boiling points of different components, the larger the difference, the easier to separate. In the meantime, operating pressure directly affects the performance of low temperature distillation. High pressure maintains the mixture completely in its critical state, thus lowering the possibility of separation. On the contrary, if the operating pressure is too low, then a large amount of refrigeration energy is required to maintain a low temperature at the top of the column.

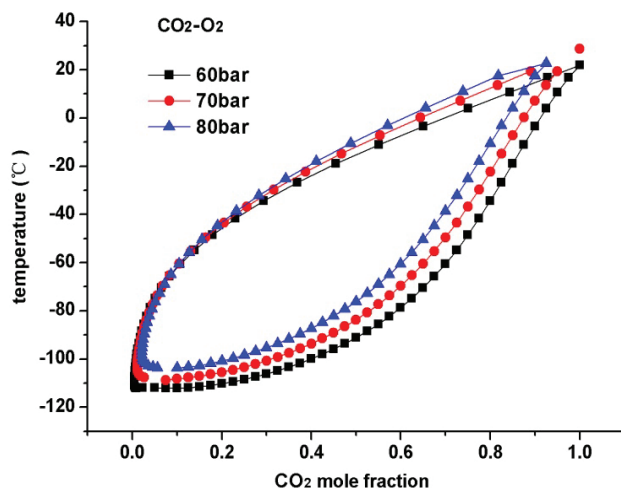
Another fundamental condition of separating a mixture by conventional distillation is that it does not form azeotropes. In the temperature-composition diagram of an azeotrope, the vapor curve is tangent to the liquidus, this point of tangency is called the azeotropic point. Neither partial vaporization nor partial condensation can change the chemical composition of an azeotropic mixture at boiling point. That is, conventional distillation is not suitable for purifying azeotropic mixtures near their boiling point.

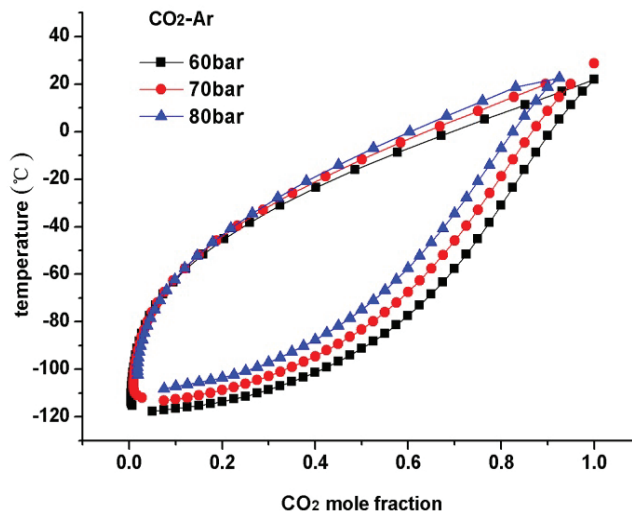
Figures 4, 5, and 6 present the temperature-composition diagrams of CO<sub>2</sub>-N<sub>2</sub>, CO<sub>2</sub>-O<sub>2</sub>, and CO<sub>2</sub>-Ar mixtures, respectively. The following conclusions can be drawn based on the figures: (1) The differences in the boiling points of CO<sub>2</sub> and other impurities (*i.e.*, N<sub>2</sub>, O<sub>2</sub>, and Ar) are still very large, even under high pressure; (2) For CO<sub>2</sub>-N<sub>2</sub>, CO<sub>2</sub>-O<sub>2</sub>, and CO<sub>2</sub>-Ar mixtures, no azeotropic point is found under high pressure conditions, hence, purifying a CO<sub>2</sub> mixture consisting of impurities such as N<sub>2</sub>, O<sub>2</sub>, and Ar via conventional distillation is feasible. The distillation process can also be conducted under high pressure and near ambient temperature conditions, which ensures a low energy penalty.

**Figure 4.** Temperature-composition diagram of CO<sub>2</sub>-N<sub>2</sub>.



**Figure 5.** Temperature-composition diagram of CO<sub>2</sub>-O<sub>2</sub>.



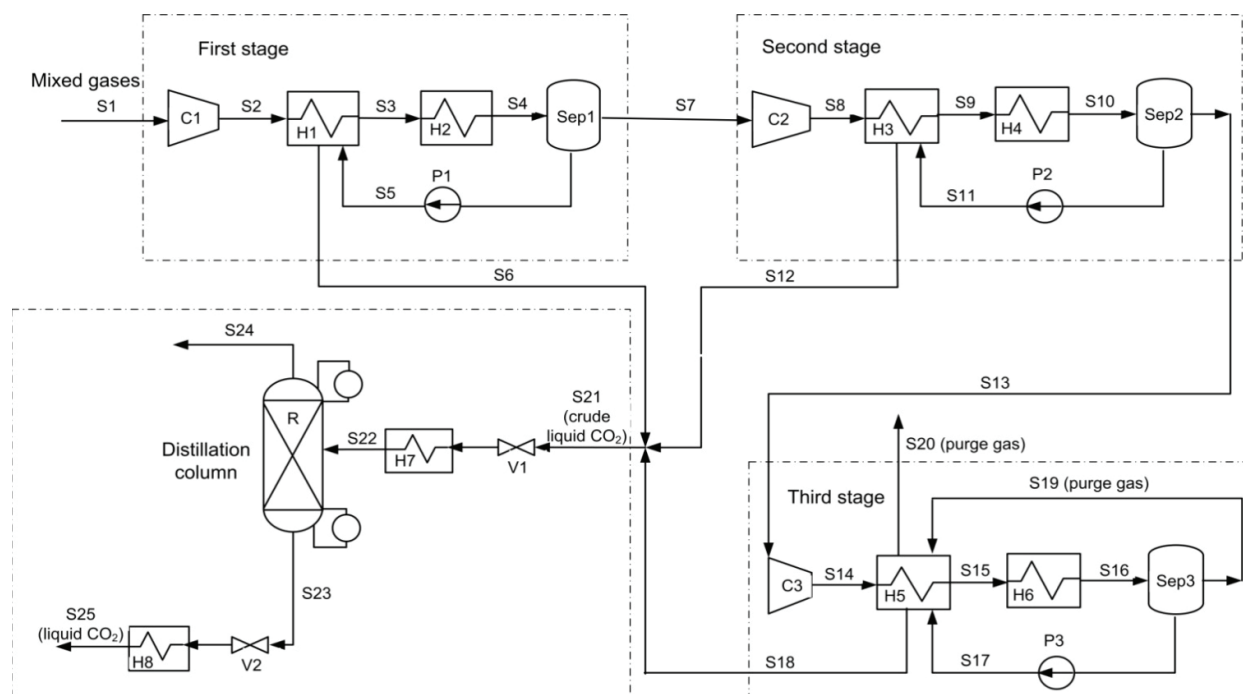
**Figure 6.** Temperature-composition diagram of CO<sub>2</sub>-Ar.

#### 4. Proposal and Performance Analysis of the Improved Separation and Purification System

##### 4.1. Schematic Diagram of the Improved Separation and Purification System

Based on the analysis above, an improved CO<sub>2</sub> separation and purification system is proposed. The whole system is made up of two subsystems: the cryogenic separation subsystem and the distillation subsystem. According to the traditional cryogenic separation method, the liquefaction temperature increases by improving the initial pressure of the mixed gases. The separation ratio could also be maintained at a high level by multi-stage separation and compression. In the distillation subsystem, crude product is distilled under high pressure and near ambient temperature conditions. Figure 7 shows the schematic diagram of this improved system.

An initial dehydration of the mixed gases is performed before they are fed into the proposed system: by cooling down to near ambient temperature, the majority of H<sub>2</sub>O is condensed and can be extracted out afterwards, while the rest is absorbed by a high-efficiency adsorbent (e.g., molecular sieve) [37]. As illustrated in Figure 7, when the dehydrated mixed gases (Stream 1 or S1) undergo the cryogenic separation and liquefaction processes, they are first compressed to an appropriate pressure (S2) by compressor 1 (C1). After cooling by the separation product, they would be cooled to a lower temperature by the external cold energy (S3). At this point, a part of the CO<sub>2</sub> is liquefied from the mixed gases. Using a gas-liquid separator (Sep1), we can separate the CO<sub>2</sub> from the mixture (S4) and pressurize it with a pump (P1). Then, part of the cold energy of the separated CO<sub>2</sub> (S5) is recovered back to the system by a heat exchanger (H1) with the mixed gases (S2) and leaves the system (S6). The abovementioned steps comprise the first stage of the process. If the mixed gases (S7) from the first stage could not satisfy the separation requirement, they are then separated in the second or the third stages. The processes of the next two stages are similar to the first one. In the cryogenic separation subsystem, three-stage separation and liquefaction are employed. When most of the CO<sub>2</sub> is separated, the purge gas (S20) leaves the system after its cold energy is recycled by a heat exchanger (H5).

**Figure 7.** Improved CO<sub>2</sub> separation and purification system.

The crude liquid CO<sub>2</sub> (S21) separated from the cryogenic separation subsystem is further purified in the distillation subsystem to improve its CO<sub>2</sub> purity. Before distillation, it is adjusted by a pressure regulating valve (V1) and a heat exchanger (H7). Temperatures on top and at the bottom of the distillation column (R) are precisely regulated within the range of  $-20\text{ }^{\circ}\text{C}$  to  $20\text{ }^{\circ}\text{C}$  and  $-10\text{ }^{\circ}\text{C}$  to  $30\text{ }^{\circ}\text{C}$ , respectively. After adjustment by the pressure regulating valve (V2) and heat exchanger (H8), the CO<sub>2</sub> product with high purity (S25) is finally obtained. V1, V2, H7, and H8 can realize pressure and temperature adjustments to a small extent, thereby ensuring that the distillation process proceeds even in abnormal working conditions, such as start and stop. However, these adjustments are not necessarily needed in normal working conditions.

#### 4.2. Simulations and Results Analysis

In this study, process simulation is conducted by ASPEN PLUS<sup>TM</sup>. The thermodynamic properties of the mixed gases are calculated by the PRMHV2 equations, because the prediction of the PRMHV2 equation can reflect the corresponding change trend of the mixture system when the initial parameters change, especially for nonpolar gas systems. The compressor and pump efficiencies are assumed to be 0.8, and the smallest temperature difference of the low-temperature heat exchanger is set at  $2\text{ }^{\circ}\text{C}$ .

Table 1 illustrates the main streams corresponding to Figure 7. As can be seen, after multi-stage compression, refrigeration, and separation, 92% of the CO<sub>2</sub> can be separated from the mixed gases in liquid state. The CO<sub>2</sub> concentrations of the crude liquid reaches 96.9%, at a pressure of 80 bar (S21). After distillation and adjustments in parameters, the CO<sub>2</sub> concentration in the final product is greatly improved to 99.9%, with the pressure decreasing to 60 bar (S23), which is suitable for most industrial applications as well as transport and storage.

**Table 1.** Parameters of the main points of the improved CO<sub>2</sub> separation and purification system.

Flow	Temperature (°C)	Pressure (bar)	Mass Flow (kg/s)	Mole Fraction (%)			
				CO <sub>2</sub>	N <sub>2</sub>	O <sub>2</sub>	Ar
S1	30.0	5	100.00	80.0	10.0	5.0	5.0
S2	30.0	21	100.00	80.0	10.0	5.0	5.0
S3	-26.5	21	100.00	80.0	10.0	5.0	5.0
S4	-35.0	21	100.00	80.0	10.0	5.0	5.0
S5	-29.7	80	62.93	98.5	0.4	0.5	0.6
S6	8.3	80	62.93	98.0	0.6	0.7	0.7
S7	-40.0	21	37.07	53.2	23.9	11.4	11.5
S8	10.4	38	37.07	53.2	23.9	11.4	11.5
S9	-25.0	38	37.07	53.2	23.9	11.4	11.5
S10	-40.0	38	37.07	53.2	23.9	11.4	11.5
S11	-31.0	80	13.35	93.8	2.1	2.1	2.0
S12	3.4	80	13.35	93.8	2.1	2.1	2.0
S13	-40.0	38	23.74	34.2	34.1	15.8	15.9
S14	-0.7	60	23.74	34.2	34.1	15.8	15.9
S15	-31.0	60	23.74	34.2	34.1	15.8	15.9
S16	-35.0	60	23.74	34.2	34.1	15.8	15.9
S17	-36.1	80	3.53	88.0	4.3	3.9	3.8
S18	-3.3	80	3.53	88.0	4.3	3.9	3.8
S19	-40.0	60	20.19	26.5	38.4	17.5	17.6
S20	-3.3	60	20.19	26.5	38.4	17.5	17.6
S21	7.3	80	79.81	96.9	1.1	1.1	1.0
S22	30.0	80	79.81	96.9	1.1	1.1	1.0
S23	22.5	60	76.18	99.9	9 ppm	48 ppm	27 ppm
S24	-10.8	60	3.62	40.5	20.1	20.0	19.3

The analysis data of the energy penalty for CO<sub>2</sub> recovery, along with some other performance parameters are summarized in Table 2. Note that the results and analysis of Table 2 are valid exclusively for the proposed system, which could be considered as polishing process instead of an intact CO<sub>2</sub> capture system, since the energy consumption of obtaining high CO<sub>2</sub> concentration is not taken into account here.

The proposed system clearly has excellent performance. The CO<sub>2</sub> recovery ratio is 90.04% with 99.9% CO<sub>2</sub> purity in the product, the energy penalty for the cryogenic separation subsystem is 29.77 MW, out of which C1, C2, and C3 consume 11.40, 2.21 and 0.72 MW, respectively; the total energy consumption for refrigeration is 18.34 MW (13.75, 3.41 and 1.18 MW for H2, H4 and H6); the total energy consumption for pumps is 0.519 MW (0.44, 0.07 and 0.009 MW for P1, P2 and P3, respectively), with 3.42 MW recovered by expansion; and the energy consumption of distillation is only 2.61 MW. In summary, the total energy penalty for this improved system is 32.38 MW, and the specific energy consumption for CO<sub>2</sub> capture is only 0.425 MJ/kgCO<sub>2</sub>.

**Table 2.** Thermodynamic performance of the improved CO<sub>2</sub> separation and purification system.

Items	Value	Unit
Mass flux of mixed gases fed to the system	100	kg/s
Mole fraction of CO <sub>2</sub> fed to the system	80	%
Mass flux of CO <sub>2</sub> fed to the system	84.62	kg/s
Mass flux of captured CO <sub>2</sub>	76.18	kg/s
CO <sub>2</sub> purity in product	99.9	%
CO <sub>2</sub> recovery ratio	90.04	%
Energy penalty for cryogenic separation subsystem	29.77	MW
Energy consumption for distillation subsystem	2.61	MW
Total energy penalty for improved system	32.38	MW
Specific energy consumption for CO <sub>2</sub> capture	0.425	MJ/kgCO <sub>2</sub>

The excellent performance of the proposed system can be attributed to its delicate process design, which is associated with highly mature technologies. The process and structural characteristics of the improved system are listed below:

- (1) Compression, refrigeration, and cryogenic separation are carried out several times in the system. Despite the fact that CO<sub>2</sub> concentration decreases continuously with CO<sub>2</sub> condensation, it can be improved by the increasing of the initial pressure, in order to maintain CO<sub>2</sub> liquefaction temperature at a high level. This condition in turn lowers the energy penalty for the cryogenic separation subsystem.
- (2) The distillation process is conducted under high pressure and near ambient temperature conditions. It can take full advantage of the large differences between the physical properties of the CO<sub>2</sub> and its impurities. It also connects perfectly with the cryogenic separation subsystem because the crude liquid CO<sub>2</sub> are under the same conditions. Consequently, the specific energy consumption for CO<sub>2</sub> capture could be as low as 0.425 MJ/kgCO<sub>2</sub>.
- (3) As a result of the distillation process, the CO<sub>2</sub> purity in the product increases dramatically and finally meets the requirements for transport and storage. Note that higher CO<sub>2</sub> purity can be expected with simple parameter improvements, such as an increase in the number of distillation trays or an enhancement of the stripping rate. The final CO<sub>2</sub> product obtained by the proposed system then becomes available to special industries (e.g., food industry), thus enhancing its additional value.

## 5. Techno-Economic Analysis of the Proposed System

### 5.1. Component Overnight Cost Estimation

Given that our proposed system is similar to the cryogenic air separation unit (ASU), the reference data for component overnight cost estimation are gathered from the literature on ASU to ensure the calculation's accuracy and validity [38–41]. The calculation methodology employed to estimate the component overnight costs follows the method used by Holt and Kreutz in studies comparing alternative IGCC systems based on a series of EPRI-sponsored studies. The present work applies the overnight cost, which includes installation investment, balance of plant, general facilities costs, engineering fees, and contingencies [42,43]. Detailed reference data are listed in Table 3.

**Table 3.** Reference data for component overnight cost estimation.

Component	Scaling parameter	C <sub>0</sub> (M\$)	S <sub>0</sub>	f	n <sup>d</sup>	Notes
Compressor	Compression power	6.3	10 MWe	0.67	1	a
Heat exchanger	MAF coal input (LHV)	39.8	1377 MWth	0.67	1	a
Separator	Inlet flow rate	0.5	71250 ton/year	0.67	1	b
Distillation column	Inlet flow rate	0.12	17600 ton/year	0.67	1	c
Pump	Outlet pressure	0.093	80 bar	0.67	1	b

a: Costs taken from Agahi [38] and Lozza and Chiesa [39]; b: Gas-liquid separator is applied here; costs taken from El-Enin [40]; c: Data taken from Haas [41]; d: n = 1 for all components in the proposed system.

In general, the overnight component cost is the function of its own size. The overnight cost of a specific component can be obtained by the following equation:

$$C = nC_0 \left[ \frac{S}{(nS_0)} \right]^f \quad (1)$$

where  $C_0$  is the overnight cost of a single train reference component whose size is  $S_0$ ;  $C$  is the overnight cost of a component whose size is  $S$ ;  $n$  is the number of equally sized trains operating at a capacity of 100%/n, and  $f$  is the scale factor.

### 5.2. Total Plant Investment

Total plant investment (TPI) is calculated as follows: TPI = total overnight cost (TOC) + interest during construction (IDC) [43]. According to Equation (1) and detailed parameters, overnight costs of major plant components are presented in Table 4. Notably, equipment made in China is generally much cheaper than that made in Western countries, essentially because of the low labor cost in China, as presented in literature [44–46].

**Table 4.** Summary of TPI calculation.

Overnight costs of plant components (M\$)	Value
C1	3.295
C2	1.767
C3	1.061
Heat Exchangers (H1–H8)	8.800
Sep1	3.747
Sep2	1.923
Sep3	1.425
Pumps (P1–P3)	0.279
Distillation Column (R)	3.825
Pipeline	2.500 <sup>e</sup>
Auxiliaries ( <i>i.e.</i> , valves)	1.250 <sup>f</sup>
TOC	29.872
IDC	3.674
TPI	33.546
Annual O&M	1.342

e, f: Overnight costs for pipeline and auxiliaries are estimated to be approximately 8% and 4% of TOC, respectively.

The main economic analysis assumptions employed in this work are: (1) The lifespan of the proposed system is assumed to be 20 years with annual working hours set at 6000 h/year [47]; (2) IDC is taken as 12.3% of TOC based on a four-year construction schedule with equal annual payments and a real discount rate ( $k$ ) of 10%/year; (3) The annual operation and maintenance cost (O&M) takes over 4% of TPI; (4) CO<sub>2</sub> transport and storage is charged for 5\$/ton, no extra carbon emission tax is attached.

The summary of the TPI calculation is shown in Table 4. TOC is 29.872 M\$ when major components and necessary auxiliaries such as pipelines and valves are considered. IDC is 3.674 M\$. The TPI of the proposed system is 33.546 M\$, and the annual O&M cost is 1.342 M\$.

Table 5 presents a brief performance comparison of several CO<sub>2</sub> recovery processes, including MEA absorption, Selexol<sup>TM</sup> absorption, and the proposed system. The techno-economic data of the MEA and Selexol<sup>TM</sup> absorption processes are collected from the IPCC report and related literature. The cost of CO<sub>2</sub> capture of the proposed system is calculated using the following equation:

$$\text{cost of CO}_2 \text{ capture} = \frac{[(\text{CRF})(\text{Total capture process investment})+(\text{Annual O\&M cost})+(\text{Annual cost on electricity})]}{\text{Annual CO}_2 \text{ captured}} \quad (2)$$

where the capital recovery factor (CRF) is related to the discounted rate ( $k$ ) and the lifespan of the system ( $l$ ); CRF is calculated as:

$$\text{CRF} = [k \cdot (1+k)^l] / [(1+k)^l - 1] \quad (3)$$

According to the previous calculation assumptions, CRF is equal to 0.117, whereas the total capture process investment and annual O&M cost are calculated based on Tables 2 to 5.

**Table 5.** Brief comparison of the techno-economic performance of several CO<sub>2</sub> recovery processes.

Items	Improved separation and purification system	MEA absorption process <sup>g</sup>	Selexol <sup>TM</sup> absorption process <sup>h</sup>
<b>Mole fractions of flue gas</b>			
CO <sub>2</sub> (%)	80.00	13.30	29.14
N <sub>2</sub> (%)	10.00	68.12	2.37
O <sub>2</sub> (%)	5.00	3.81	0.00
Ar (%)	5.00	3.50	0.43
H <sub>2</sub> O (%)	—	11.25	26.38
H <sub>2</sub> (%)	—	—	40.13
Other (%)	—	0.02	1.55
<b>Techno-economic indicators</b>			
Mass flux of captured CO <sub>2</sub> (kg/s)	76.18	113.33	66.83
CO <sub>2</sub> recovery ratio (%)	90.04	90.0	87
CO <sub>2</sub> purity in product (%)	99.9	98	95
Total energy penalty (MW)	32.38	441.9	62
Energy penalty for recovering unit CO <sub>2</sub> (MJ/kgCO <sub>2</sub> )	0.425	3.9	0.928
Total capture process investment (M\$)	33.546	133.470	55.8
Specific capture process investment (M\$/(kg·s <sup>-1</sup> ))	0.440	1.178	0.835
Cost of CO <sub>2</sub> capture (\$/tCO <sub>2</sub> )	10.28	24	19

g: Data taken from Abu-Zahra [48] and the IPCC report (2007) [2]; h: Data taken from the IPCC report (2007) [2] and NETL (2002) [49].

As shown in Table 5, the specific capture process investment of the improved system is only  $0.440 \text{ M}\$/(\text{kg}\cdot\text{s}^{-1})$ , and its cost of  $\text{CO}_2$  capture is  $10.28 \text{ \$/tCO}_2$ . As for the MEA and Selexol<sup>TM</sup> absorption methods, the specific capture process investments are  $1.178 \text{ M}\$/(\text{kg}\cdot\text{s}^{-1})$  and  $0.835 \text{ M}\$/(\text{kg}\cdot\text{s}^{-1})$ , respectively, whereas their costs of  $\text{CO}_2$  capture increase to  $24 \text{ \$/tCO}_2$  and  $19 \text{ \$/tCO}_2$ , respectively. Which means compared to conventional MEA and Selexol<sup>TM</sup> absorption methods, the cost of  $\text{CO}_2$  capture of the proposed system reduces by 57.2% and 45.9%, respectively.

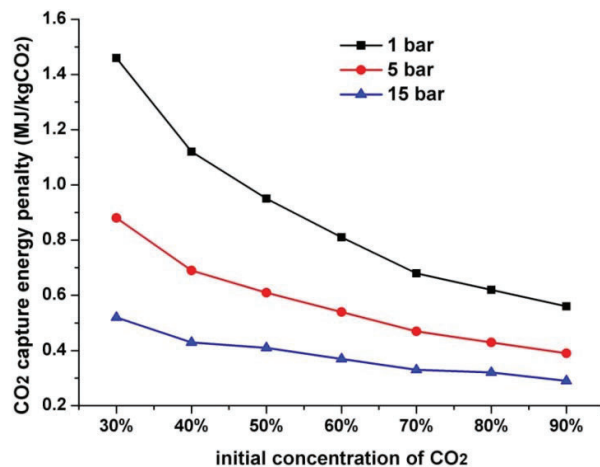
Note that the cost data found in related literature varies widely due to different estimation methods, design requirements, construction materials, and national conditions. Different recovery processes are applicable to various flue gas compositions, as revealed in Table 5. Hence, the improved system is not necessarily much better than or able to replace conventional absorption processes. We try to demonstrate in this study that if the initial  $\text{CO}_2$  concentration of the gas mixture is relatively high (e.g., oxy-fuel combustion or pre-combustion capture), then the proposed system provides a feasible and competitive approach to  $\text{CO}_2$  capture with respect to thermodynamic and economic performance. Briefly, performance of the proposed system in combination with oxy-fuel combustion is evaluated. The amount of oxygen needed for oxy-fuel combustion is roughly  $65.4\text{--}75.7 \text{ kg/s}$  according to the law of conservation of mass, the energy consumption and additional investment of air separation unit are about  $39\text{--}44 \text{ MW}$  and  $39\text{--}42 \text{ M}\$$  with reference to related bibliography [44,50,51]. As a result, the total energy penalty for  $\text{CO}_2$  capture will increase from  $0.425 \text{ MJ/kgCO}_2$  to  $0.937\text{--}1.003 \text{ MJ/kgCO}_2$ , specific capture process investment will increase from  $0.440 \text{ M}\$/(\text{kg}\cdot\text{s}^{-1})$  to  $0.952\text{--}0.992 \text{ M}\$/(\text{kg}\cdot\text{s}^{-1})$ , and cost of  $\text{CO}_2$  capture will rise from  $10.28 \text{ \$/tCO}_2$  to approximately  $18.32\text{--}18.60 \text{ \$/tCO}_2$ .

## 6. Discussion

### 6.1. Influences of Initial Pressure and Initial Concentration on the $\text{CO}_2$ Capture Energy Penalty

The initial pressure and initial concentration of the mixed gases have a great influence on the performance of the proposed system. Figure 8 presents the relationship between the  $\text{CO}_2$  capture energy penalty against its initial pressure and concentration.

**Figure 8.** Relationship between  $\text{CO}_2$  capture energy penalty against initial pressure and concentration.



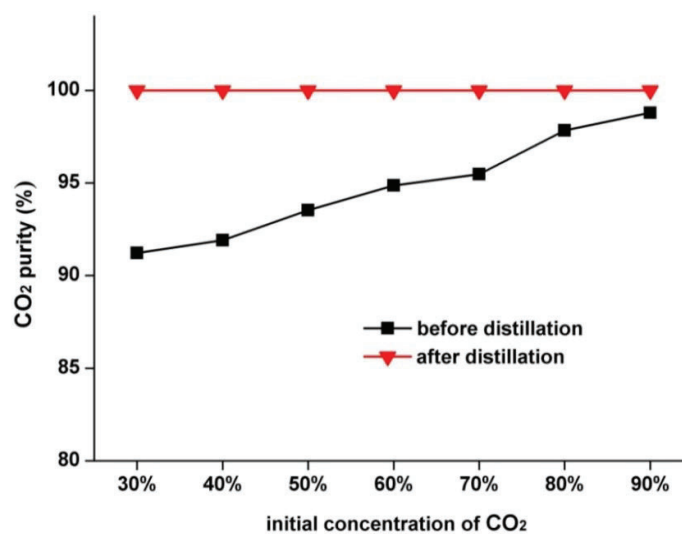
As shown in the curves, the energy penalty for CO<sub>2</sub> capturing unit greatly decreases with the increase in the initial pressure. In the proposed system, the mixed gases must first be compressed into a relatively high pressure to keep the liquefaction temperature at a high level, thus compression work of the first stage is relatively high and could consume over 30% to 50% of the total energy penalty. If the initial pressure of the mixed gases is relatively high at the beginning, lots of compression work could be saved for the first stage. The result is a decrease in the CO<sub>2</sub> capture energy penalty.

The CO<sub>2</sub> capture energy penalty also decreases substantially due to the increase of initial CO<sub>2</sub> concentration. As shown in Figure 8, the CO<sub>2</sub> capture energy penalty at an initial concentration of 60% increases by approximately 50% compared with that at an initial concentration of 80% in a fixed initial pressure. This value increases by approximately 150% when the initial concentration is 40%. This condition is due to in low initial CO<sub>2</sub> concentration, large refrigeration work is required to deal with the low liquefaction temperature. If the initial CO<sub>2</sub> concentration is enhanced, the CO<sub>2</sub> capture energy penalty will decrease significantly. In summary, the proposed system has superior performance in recovering CO<sub>2</sub> from mixed gases with high initial CO<sub>2</sub> concentration and initial pressure.

### 6.2. CO<sub>2</sub> Purity Comparison before and after Distillation

If the initial CO<sub>2</sub> concentration in the CO<sub>2</sub>-N<sub>2</sub> mixture changes, the CO<sub>2</sub> purity in the final product obtained through the cryogenic separation method varies. Figure 9 provides the relationship between CO<sub>2</sub> purity and initial concentration of CO<sub>2</sub> before and after distillation. The CO<sub>2</sub> purity in the product is relatively low before distillation, although it is improved as the initial CO<sub>2</sub> concentration increases. Specifically, CO<sub>2</sub> purity without distillation is only 92% at an initial concentration of 30% and reaches only 98.78% at an initial CO<sub>2</sub> concentration of 90%. By contrast, the CO<sub>2</sub> purity in the product is constantly above 99.9% after distillation regardless of the initial CO<sub>2</sub> concentration. At this level, the CO<sub>2</sub> purity perfectly meets the requirements for most industrial applications as well as transport and storage. The distillation process can significantly improve the CO<sub>2</sub> purity in the product, thus proving that it is an effective and necessary purification method for separating CO<sub>2</sub>-N<sub>2</sub> mixture.

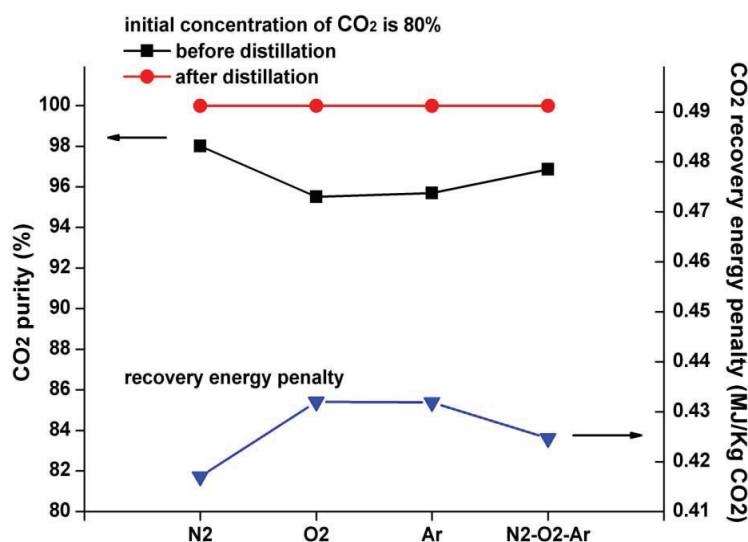
**Figure 9.** CO<sub>2</sub> purity comparison before and after distillation.



### 6.3. Analysis of the CO<sub>2</sub> Purity in the Product with Different Initial Compositions

Figure 10 shows the influences of different initial compositions on CO<sub>2</sub> purity and CO<sub>2</sub> recovery energy penalty. Supposing the initial CO<sub>2</sub> concentration of the mixed gases is 80%, four kinds of typical initial compositions are discussed: N<sub>2</sub>, O<sub>2</sub>, Ar, and N<sub>2</sub>-O<sub>2</sub>-Ar. The concentrations of these components are equally set at 20%. For N<sub>2</sub>-O<sub>2</sub>-Ar, the concentration of each component is 10%, 5%, and 5%, respectively. As can be seen, before distillation, the CO<sub>2</sub> purity is greatly affected by the change in initial composition. For N<sub>2</sub>, O<sub>2</sub>, Ar, and N<sub>2</sub>-O<sub>2</sub>-Ar, their CO<sub>2</sub> purities without distillation are only 98.01%, 95.5%, 95.69%, and 96.86%, respectively. After distillation, the CO<sub>2</sub> purity increases to more than 99.9% for all circumstances. The recovery energy penalty fluctuates within the range of 5% when the initial composition varies, which demonstrates that the proposed system presents excellent performance for various initial compositions.

**Figure 10.** Influences of different initial compositions on CO<sub>2</sub> purity and CO<sub>2</sub> recovery energy penalty.



## 7. Conclusions

Based on an in-depth analyses of cryogenic separation and distillation theory as well as the phase transition characteristics of gas mixtures containing CO<sub>2</sub>, this study presents an improved CO<sub>2</sub> separation and purification system. According to the theoretical analysis, case simulations, and regularity analysis discussed above, the following conclusions are drawn:

- (1) By adopting multi-stage compression, refrigeration, and separation, the resulting improved cryogenic separation subsystem could separate the majority of CO<sub>2</sub> from gas mixtures with relatively low energy penalty and could fully recover the cold energy of the separation product.
- (2) Considering the large difference between the physical properties of CO<sub>2</sub> and other impurities, the distillation process is conducted under high pressure and near ambient temperature conditions. Consequently, the CO<sub>2</sub> purity in the product significantly increases to more than

99.9%, whereas the energy penalty for distillation is rather low. This condition finally realizes the low energy penalty of purification.

- (3) The cost of CO<sub>2</sub> capture of the proposed system is much lower than those of conventional absorption methods, because it mainly adopts common equipment which are widely utilized and highly mature in the chemical industry (e.g., compressors, heat exchangers, and pumps). Besides, this equipment can operate effectively for a long term under comparatively mild working condition as there is no serious corrosion or secondary pollution problems. Consequently, the TPI and annual O&M could be maintained at low levels.
- (4) The proposed system has superior performance in recovering CO<sub>2</sub> from mixed gases with high initial CO<sub>2</sub> concentration. Note that the high initial pressure of mixed gases contributes to lowering the CO<sub>2</sub> recovery energy penalty. Furthermore, the analysis proves that the proposed system can efficiently recover CO<sub>2</sub> from mixed gases, regardless of initial compositions as the CO<sub>2</sub> purity in the product could be as high as 99.9% under various circumstances.

## Acknowledgments

This study was supported by the National Nature Science Fund of China (No. 51025624), National Key Technology R&D Program of China (2012BAC24B01), the 111 Project (B12034), and the Fundamental Research Funds for the Central Universities (2014ZD04).

## Author Contributions

In this paper, Gang Xu provided the original idea and constructs its framework, and was responsible for drafting and revising the whole paper; Feifei Liang conducted the detailed calculation, simulation and contributes to revising the paper; Yongping Yang was the main technical guidance; Yue Hu devoted efforts to the writing of the techno-economic analysis in Section 5.1, and gave some valuable comments on revising the paper; Kai Zhang wrote the bulk of the distillation mechanism in Section 3.1; Wenyi Liu completed the further discussion of the proposed system in Section 6.2. All authors read and approved the manuscript.

## Conflicts of Interest

The authors declare no conflict of interest.

## References

1. Working Group III of the Intergovernmental Panel on Climate Change (IPCC). *IPCC Special Report on Carbon Dioxide Capture and Storage*; Cambridge University Press: Cambridge, UK, 2005.
2. Working Group III of the Intergovernmental Panel on Climate Change (IPCC). *IPCC's Fourth Assessment Report (AR4): Mitigation of Climate Change*; Cambridge University Press: Cambridge, UK, 2007.
3. Ma'mun, S.; Svendsen, H.F.; Hoff, K.A.; Juliussen, O. Selection of new absorbents for carbon dioxide capture. *Energy Convers. Manag.* **2007**, *48*, 251–258.

4. Saha, A.K.; Biswas, A.K.; Bandyopadhyay, S.S. Absorption of CO<sub>2</sub> in a sterically hindered amine: Modeling absorption in a mechanically agitated contactor. *Sep. Purif. Technol.* **1999**, *15*, 101–112.
5. Mandal, B.P.; Guha, M.; Biswas, A.K.; Bandyopadhyay, S.S. Removal of carbon dioxide by absorption in mixed amines: Modeling of absorption in aqueous MDEA/MEA and AMP/MEA solutions. *Chem. Eng. Sci.* **2001**, *56*, 6217–6224.
6. Alie, C.; Backham, L.; Croiset, E.; Douglas, P.L. Simulation of CO<sub>2</sub> capture using MEA scrubbing: A flowsheet decomposition method. *Energy Convers. Manag.* **2005**, *46*, 475–487.
7. Dorctor, R.D.; Molburg, J.C.; Thimmapuram, P.R. *Gasification Combined Cycle: Carbon Dioxide Recovery, Transport, and Disposal*; ANL/ESD-24; Argonne National Laboratory: Argonne, IL, USA, 1994.
8. Dorctor, R.D.; Molburg, J.C.; Thimmapuram, P.R. *KRW Oxygen-blown Gasification Combined Cycle: Carbon Dioxide Recovery, Transport, and Disposal*; ANL/ESD-34; Argonne National Laboratory: Argonne, IL, USA, 1996.
9. Zhang, J.; Webley, P.A.; Xiao, P. Effect of process parameters on power requirements of vacuum swing adsorption technology for CO<sub>2</sub> capture from flue gas. *Energy Convers. Manag.* **2008**, *49*, 346–356.
10. Na, B.K.; Koo, K.K.; Eum, H.M. CO<sub>2</sub> Recovery from flue gas by PSA process using activated carbon. *Korean J. Chem. Eng.* **2001**, *18*, 220–227.
11. Siriwardane, R.V.; Shen, M.S.; Fisher, E.P. Adsorption of CO<sub>2</sub> on molecular sieves and activated carbon. *Energy Fuels* **2001**, *15*, 279–284.
12. Siriwardane, R.V.; Shen, M.S.; Fisher, E.P. Adsorption of CO<sub>2</sub>, N<sub>2</sub>, and O<sub>2</sub> on natural zeolites. *Energy Fuels* **2003**, *17*, 571–576.
13. Gomes, V.G.; Yee, K.W.K. Pressure swing adsorption for carbon dioxide sequestration from exhaust gases. *Sep. Purif. Technol.* **2002**, *28*, 161–171.
14. Yan, S.P.; Fang, M.X.; Zhang, W.F.; Zhong, W.L.; Luo, Z.Y.; Cen, K.F. Comparative analysis of CO<sub>2</sub> separation from flue gas by membrane gas absorption technology and chemical absorption technology in China. *Energy Convers. Manag.* **2008**, *49*, 3188–3197.
15. Powell, C.E.; Qiao, G.G. Polymeric CO<sub>2</sub>/N<sub>2</sub> gas separation membranes for the capture of carbon dioxide from power plant flue gases. *J. Membr. Sci.* **2006**, *279*, 1–49.
16. Feron, P.H.M.; Jansen, A.E. CO<sub>2</sub> separation with polyolefin membrane contactors and dedicated absorption liquids: Performances and prospects. *Sep. Purif. Technol.* **2002**, *27*, 231–242.
17. Pierce, W.F.; Riemer, P.; William, G.O. International perspectives and the results of carbon dioxide capture disposal and utilisation studies. *Energy Convers. Manag.* **1995**, *36*, 813–818.
18. Wang, B.Q. *Process Mechanism and System Synthesis for CO<sub>2</sub> Capture in IGCC System*; Chinese Academy of Sciences: Beijing, China, 2004.
19. Wang, B.Q.; Jin, H.G.; Han, W. IGCC system with integration of CO<sub>2</sub> recovery and the cryogenic energy in air separation unit. In Proceedings of ASME Turbo Expo, Vienna, Austria, 14–17 June 2004; GT-2004-53723.
20. Wang, B.Q.; Jin, H.G. A novel IGCC system with H<sub>2</sub>/O<sub>2</sub> cycle and CO<sub>2</sub> recovery by ASU cryogenic energy. In Proceedings of the 7th International Conference on Greenhouse Gas Control Technologies, Vancouver, BC, Canada, 5–9 September 2004.

21. Deng, S.; Jin, H.; Cai, R. Novel cogeneration power system with LNG cryogenic exergy utilization. *Energy* **2004**, *29*, 497–512.
22. Zhang, N.; Lior, N. A novel near-zero CO<sub>2</sub> emission thermal cycle with LNG cryogenic exergy utilization. *Energy* **2006**, *31*, 1666–1679.
23. Song, C.F.; Kitamura, Y.; Li, S.H. Evaluation of Stirling cooler system for cryogenic CO<sub>2</sub> capture. *Appl. Energy* **2012**, *98*, 491–501.
24. Kanniche, M.; Gros-Bonnivarda, R.; Jauda, P.; Valle-Marcosa, J.; Amann, J.M.; Boualloub, C. Pre-combustion, post-combustion and oxy-combustion in thermal power plant for CO<sub>2</sub> capture. *Appl. Therm. Eng.* **2010**, *30*, 53–62.
25. Zanganeh, K.E.; Shafeen, A. A novel process integration, optimization and design approach for large-scale implementation of oxy-fired coal power plants with CO<sub>2</sub> capture. *Greenh. Gas Control* **2007**, *1*, 47–54.
26. Zanganeh, K.E.; Shafeen, A.; Salvador, C. CO<sub>2</sub> capture and development of an advanced pilot-scale cryogenic separation and compression unit. *Energy Procedia* **2009**, *1*, 247–252.
27. Li, H.; Yan, J.; Yan, J.; Anheden, M. Impurity impacts on the purification process in oxy-fuel combustion based CO<sub>2</sub> capture and storage system. *Appl. Energy* **2009**, *86*, 220–213.
28. Besong, M.T.; Maroto-Valer, M.M.; Finn, A.J. Study of design parameters affecting the performance of CO<sub>2</sub> purification units in oxy-fuel combustion. *Int. J. Greenh. Gas Control* **2013**, *12*, 441–449.
29. Song, C.F.; Kitamura, Y.; Li, S.H.; Jiang, W.Z. Analysis of CO<sub>2</sub> frost formation properties in cryogenic capture process. *Int. J. Greenh. Gas Control* **2013**, *13*, 26–33.
30. Jana, A.K. Heat integrated distillation operation. *Appl. Energy* **2010**, *87*, 1477–1494.
31. Xu, G.; Li, L.; Yang, Y.P.; Tian, L.H.; Liu, T.; Zhang, K. A novel CO<sub>2</sub> cryogenic liquefaction and separation system. *Energy* **2012**, *42*, 522–529.
32. Xu, G.; Jin, H.G.; Yang, Y.P.; Duan, L.Q.; Han, W.; Gao, L. A novel coal-based hydrogen production system with low CO<sub>2</sub> emissions. *ASME J. Eng. Gas Turbines Power* **2010**; *132*, 031701–031709.
33. Xu, G.; Yang, Y.P.; Duan, L.Q.; Wang, N. A novel integration method for CO<sub>2</sub> separation and compression. *J. Eng. Thermophys.* **2010**, *31*, 1643–1646. (in Chinese)
34. Humphrey, J.L.; Siebert, A.F. Separation technologies: An opportunity for energy savings. *Chem. Eng. Prog.* **1992**, *88*, 80–92.
35. Engeliën, H.K.; Skogestad, S. Selecting appropriate control variables for a heat integrated distillation system with prefractionator. *Comput. Chem. Eng.* **2004**, *28*, 683–691.
36. Al-Muslim, H.; Dincer, I. Thermodynamic analysis of crude oil distillation systems. *Int. J. Energy Res.* **2005**, *29*, 637–655.
37. Toftegaard, M.B.; Brix, J.; Jensen P.A.; Glarborg, P.; Jensen, A.D. Oxy-fuel combustion of solid fuels. *Prog. Energy Combust. Sci.* **2010**, *36*, 581–625.
38. Agahi, R. *GE Power Systems*; Rotoflow, Inc.: Gardena, CA, USA, December 2002 personal communication.

39. Lozza, G.; Chiesa, P. CO<sub>2</sub> sequestration techniques for IGCC and natural gas power plants: A comparative estimation of their thermodynamic and economic performance. In Proceedings of International Conference on Clean Coal Technologies for our Future, Chia Laguna, Italy, 21–23 October 2002.
40. El-Enin, S.A.A.; Attia, N.K.; El-Ibiari, N.N.; El-Diwani, G.I.; El-Khatib, K.M. *In-situ* transesterification of rapeseed and cost indicators for biodiesel production. *Renew. Sustain. Energy Rev.* **2013**, *18*, 471–477.
41. Haas, M.J.; McAloon, A.J.; Yee, W.C.; Foglia, T.A. A process model to estimate biodiesel production costs. *Bioresour. Technol.* **2006**, *97*, 671–678.
42. Holt, N. IGCC Power Plants—EPRI Design and Cost Studies. In Proceedings of EPRI/GTC Gasification Technologies Conference, San Francisco, CA, USA, 6 October 1998.
43. Kreutz, T.; Williams, R.; Consonni, S.; Chiesa, P. Co-production of hydrogen, electricity and CO<sub>2</sub> from coal with commercially ready technology. Part B: Economic analysis. *Int. J. Hydrog. Energy* **2005**, *30*, 769–784.
44. Huang, B.; Xu, S.S.; Gao, S.H.; Liu, L.B.; Tao, J.Y.; Niu, H.W.; Cai, M.; Cheng, J. Industrial test and techno-economic analysis of CO<sub>2</sub> capture in Huaneng Beijing coal-fired power station. *Appl. Energy* **2010**, *87*, 3347–3354.
45. Zhao, M.; Minett, A.I.; Harris, A.T. A review of techno-economic models for the retrofitting of conventional pulverised-coal power plants for post-combustion capture (PCC) of CO<sub>2</sub>. *Energy Environ. Sci.* **2013**, *6*, 25–40.
46. Huang, B.; Xu, S.S.; Gao, S.H.; Liu, L.B.; Tao, J.Y.; Niu, H.W.; Cai, M.; Cheng, J. Industrial test of CO<sub>2</sub> capture in Huaneng Beijing coal-fired power station. *Proc. CSEE* **2009**, *29*, 14–20. (In Chinese)
47. Nam, H.; Lee, T.; Lee, J.; Lee, J.; Chung, H. Design of carrier-based offshore CCS system: Plant location and fleet assignment. *Int. J. Greenh. Gas Control* **2013**, *12*, 220–230.
48. Abu-Zahra, M.R.M.; Niederer, J.P.M.; Feron, P.H.M.; Versteeg, G.F. CO<sub>2</sub> capture from power plants Part II. A parametric study of the economical performance based on mono-ethanolamine. *Int. J. Greenh. Gas Control* **2007**, *1*, 135–142.
49. Parsons, E.L.; Shelton, W.W.; Lyons, J.L. *Advanced Fossil Power Systems Comparison Study, Final Report Prepared for NETL*; National Energy Technology Laboratory: Morgantown, WV, USA, 2012.
50. Xiong, J.; Zhao, H.B.; Zheng, C.G.; Liu, Z.H.; Zeng, L.D.; Liu, H.; Qiu, J.R. An economic feasibility study of O<sub>2</sub>/CO<sub>2</sub> recycle combustion technology based on existing coal-fired power plants in China. *Fuel* **2009**, *88*, 1135–1142.
51. Doukelis, A.; Vorrias, I.; Grammelis, P.; Kakaras, E.; Whitehouse, M.; Riley, G. Partial O<sub>2</sub>-fired coal power plant with post-combustion CO<sub>2</sub> capture: A retrofitting option for CO<sub>2</sub> capture ready plants. *Fuel* **2009**, *88*, 2428–2436.